JOURNAL OF WATER AND LAND DEVELOPMENT
e-ISSN 2083-4535

Polish Academy of Sciences (PAN)
Institute of Technology and Life Sciences (ITP)

JOURNAL OF WATER AND LAND DEVELOPMENT
2021, No. 48 (I–III): 148–161; https://doi.org/10.24425/jwld.2021.136158

Available (PDF): https://www.itp.edu.pl/JWLD; http://journals.pan.pl/jwld

Received 11.05.2020
Reviewed 23.10.2020
Accepted 05.11.2020

Spatial and temporal evaluation of global rainfall products in a data-scarce region: The Dez Basin, Iran

Mostafa KHOSHCHEHREH[1)] ✉, Mehdi GHOMESHI[1)], Ali SHAHBAZI[1)], Hossein BOLBOLI[1)], Hamed SABERI[2)], Ali GORJIZADE[1)]

[1)] Shahid Chamran University of Ahvaz, Faculty of Water Science Engineering, Department of Water and Hydraulic Structures, Golestan Blvd., Ahvaz, 6135783151, Iran
[2)] Khorramshahr University of Marine Science and Technology, Faculty of Engineering, Khorramshahr, Iran

For citation: Khoshchehreh M., Ghomeshi M., Shahbazi A., Bolboli H., Saberi H., Gorjizade A. 2021. Spatial and temporal evaluation of global rainfall products in a data-scarce region: The Dez Basin, Iran. Journal of Water and Land Development. No. 48 (I–III) p. 148–161. DOI 10.24425/jwld.2021. 136158.

Abstract

The limitation in approachability to rainfall data sources with an appropriate spatial-temporal distribution is a significant challenge in different parts of the world. The development of general circulation models and mathematical algorithms has led to the generation of various rainfall products as new sources with the potential to overcome the shortage in data-scarce basins. In this study, the performance of the PERSIANN-CCS and CMORPH satellite-based rainfall product, as well as the ERA5 and ERA-Interim reanalysis, was evaluated based on detection skill and quantitative metrics in a daily, monthly and seasonal time scales in the Dez basin located in the southwest of Iran. The basin has a wide topographic variation and scattered rain gauge stations. Overall results denote that the ERA5 dataset has the best performance in all statistic verification than other rainfall products. Based on the daily evaluation of all rainfall products, the false alarm rate (*FAR*) is higher than 0.5, so none of the datasets could capture the temporal variability of rainfall occurrence. This study has covered the western parts of the Zagros steep slopes in which the topographic conditions have a significant effect on the activity of rainfall systems. On a monthly scale, the mean value of the correlation coefficient (*CC*) for ERA5, ERA-Interim, PERSIANN-CCS, and CMORPH was equal to 0.86, 0.85, 0.51, 0.39, respectively. The results of seasonal evaluation suggested that all datasets have better rainfall estimation in autumn and winter, and the capability of all datasets dramatically decreased in the spring. The current paper argues that the ERA5 reanalysis typically outperforms ERA-Interim and can be considered as a reliable rainfall source in the future hydrological investigation in the southwest of Iran.

Key words: *CMORPH, ERA5, ERA-Interim, PERSIANN-CCS, precipitation datasets, reanalysis data, satellite-based precipitation*

INTRODUCTION

The use of high-resolution rainfall data in the primary input of rainfall-runoff models may lead to the increased predictive accuracy of these models and reliability of water resource management decisions, especially in data scarce regions. The network of radar-based meteorological stations and rain gauges are used as the two primary sources of rainfall databases. The dispersion and constraints of these stations are such that in some areas of the highest rainfall per year no measuring station is found [WESTRICK *et al.* 1999]; hence, the recorded data cannot accurately reflect the distribution of rainfall. The satellite-based and reanalysis grid data (rainfall products) are not limited to rain gauges and radar-based stations, and they are available in different parts of the Earth [KUCERA *et al.* 2013]. Because of their high spatial resolution, they can be used as a complementary source for rainfall gauge and radar data [YONG *et al.* 2012]. The use of rainfall products in a data-scarce region is prevalent in hydrology, particularly as input variables in a hydrological model [KHOSHCHEHREH *et al.* 2020; SUSENO, YAMADA 2020]. Nonetheless, these da-

tasets have intrinsic uncertainties associated with the generation and utilization method [ISOTTA *et al*. 2015; PREIN, GOBIET 2017]. Therefore, to obtain reliable results useful in hydrological applications, it is indispensable to characterize the accuracy of the rainfall estimate.

In recent years, different studies have been conducted on validation of gridded rainfall estimates (rainfall products) across the world [DARAND, KHANDU 2020; NOGUEIRA 2020; TAREK *et al*. 2020]. The results of these studies showed that their performance differs in every part of the world. For example, in a study [XU *et al.* 2019] an evaluation of variability was done using different rainfall datasets, including ERA5 and ERA-Interim in Northern Great Plains. It was concluded that these products show better results in spring and fall than in summer and winter. Another study [CHEN *et al.* 2020] compared the performance of satellite-based rainfall products, including PERSIANN-CCS, around the globe and it found that missed rainfall events over humid southern regions are one of the dominant error sources in the PERSIANN-CCS dataset. SKOK *et al*. [2016] investigated the rainfall intercomparison based on data obtained from various gridded datasets, including CMORPH, TRMM, ERA-Interim reanalysis data, and a single climate simulation using the WRF model in Europe and North Atlantic. They concluded that the ERA--Interim data had a small dry bias over the land, whereas the WRF simulation had a sizeable wet bias equal to +30%, and CMORPH showed a significant and consistent dry bias of –21%. Both ERA-Interim and CMORPH products had a small wet bias of +8%, while the wet bias in the WRF was significantly larger and equal to +47% over the ocean.

In Iran, limited evaluations have been performed to determine the skill and potential of rainfall products and most of the studies in Iran were based only on the previous generation rainfall satellite datasets [DARAND *et al*. 2017; MOAZAMI *et al.* 2016]. For instance, in a work by MOAZAMI *et al.* [2013], authors evaluated daily rainfall obtained from PERSIANN, TMPA 3B42V6, and TMPA 3B42RT products in 47 rainfall events between 2003 and 2006. Results of this evaluation showed that TMPA 3B42V6, with a mean bias of –1.47 mm, had a better performance in rainfall estimation in selected events. Another study [MOAZAMI *et al.* 2016] assessed the performance of satellite rainfall products, including PERSIANN, CMORPH, and TMPA datasets under diverse climate conditions in Iran. The evaluations of different seasons indicate that the best performance for PERSIANN and TMPA products is during winter, while for CMORPH during autumn. However, the rainfall products potentiality in recent years is less addressed, particularly by reanalysis datasets such as ERA5. Most of the catchments in Iran can be considered as data-scarce, especially in the southwest (study area) where in situ rain gauges are either sparse or scarce and accessibility to rainfall data of an appropriate temporal and spatial resolution is regarded a challenge.

Flooding as a natural hazard is the dominant climatic extreme events in the southwestern parts of Iran [SAMADI *et al*. 2019]. In the last decade, a number of floods have occurred in this region. One of challenges concerning this area is the lack of the adequate rain gauge network. Besides, specific geographical conditions of this region have caused critical challenges to obtain rainfall data of an appropriate temporal and spatial resolution; hence, it is highly important to examine the potential of rainfall estimate data, such as satellite-based and reanalysis datasets.

The main research objective is to investigate the daily, monthly, and seasonal rainfall, considering validation measures, such as the spatial distribution of quantitative metrics and rainfall detection skill at the Dez Basin in the southwest of Iran. Additionally, the current study focuses on the inter-comparison of two satellite-based rainfall datasets (PERSIAN-CCS and CMORPH) and ERA5 and ERA-Interim reanalysis data with rain gauge observations over nine years between 2008 and 2017.

MATERIALS AND METHODS

STUDY AREA

The Dez Basin is located in the southwest of Iran between 10´48° and 21´50º east longitude 34´31° and 7´34° north latitudes (Fig. 1). The total area of the basin is 21720 km^2 and the maximum and minimum elevation of 4124 m and 190 m, respectively. Based on the Köppen–Geiger climate classification index [PEEL *et al*. 2007], the study area consists of two climatic zones, i.e. hot-summer Mediterranean climate (Csa) and cold semi-arid climate (Bsk). The west part of the basin is in the Csa climate zone while the east in the Bsk climate zone [RAZIEI 2016]. Precipitation in the basin appears in the form of rainfall, whereas snowfall is rare. KIANI *et al*. [2019] have shown that the moisture formation and transfer originates from the Arab and Red Seas and moves to western parts of Iran in the form of a low humidity pressure system.

The topography of the Dez Basin is complex due to the presence of the Zagros Mountains. Furthermore, the mountains are a natural barrier to Sudanese systems, establishing suitable conditions for a fast ascent of air and creation and development of cumulus clouds in the eastern and elevated parts of the Dez Basin. This leads to a major variation in rainfall on steep slopes, higher than in other areas.

The mean annual rainfall in the north and east of the study area is generally higher than in other areas. As for the temporal distribution of rainfall, 48.8% of rainfall occurs in winter, followed by 30.6% occurring in autumn, 20.4% in spring, and only 2.9% in summer (Khuzestan Water and Power Authority). Figure 2 illustrates the amount of daily and monthly rainfall data obtained from rain gauge stations from January to December in 2008–2017. In this area, the average values of monthly rainfall from November to April have been higher than in other months of the year. Furthermore, the average maximum daily rainfall corresponding to October and November is 35 and 26 mm, respectively. Moreover, the absolute maximum daily participation occurs in April and October. In contrast, the average minimum daily rainfall is recorded in summer between May and August. The mean annual distribution of rainfall occurrence with varying intensity thresholds based on the World Meteorological Organiza-

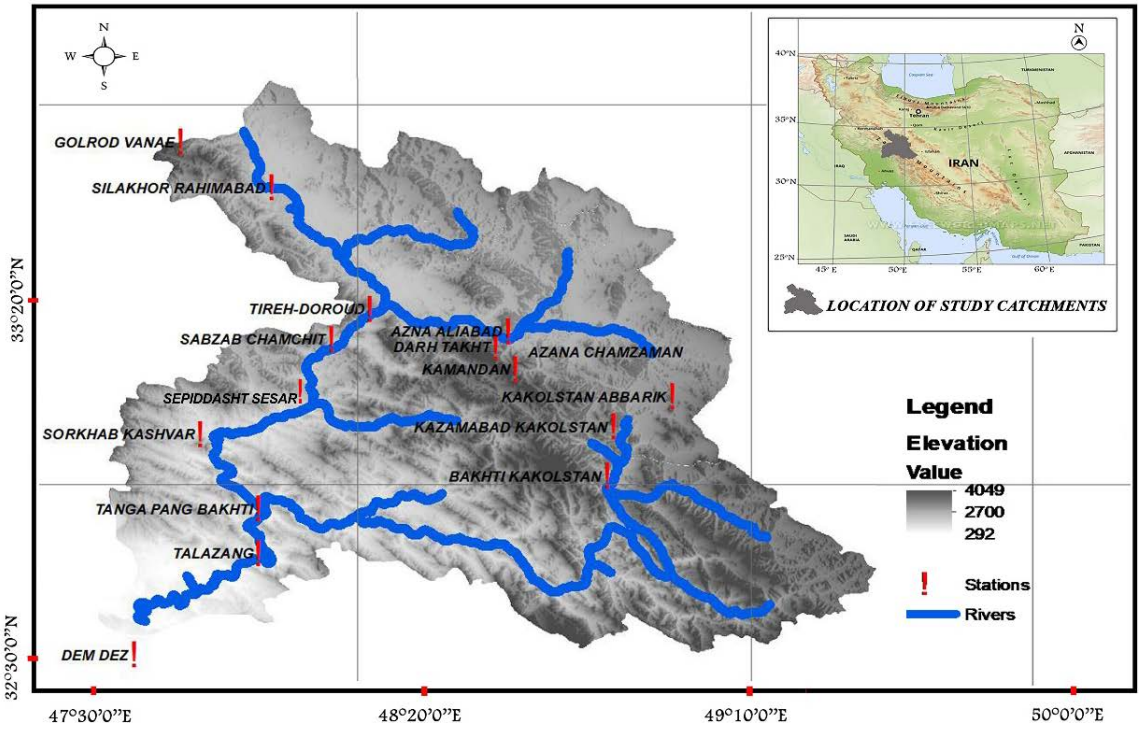

Fig. 1. The Dez River watershed and spatial distribution of rain gauges; source: own elaboration

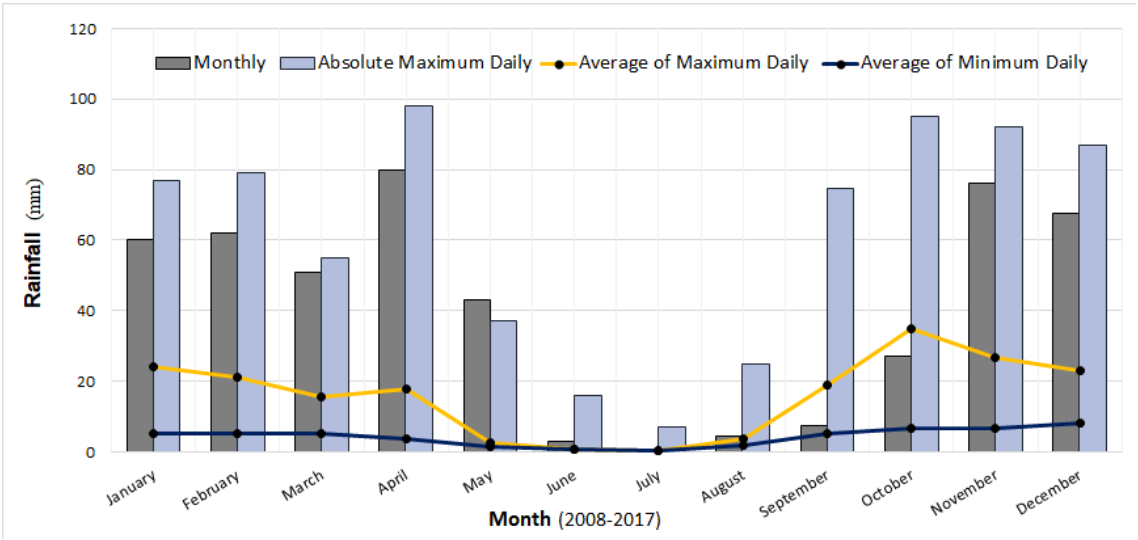

Fig. 2. Daily and monthly rainfall data from rain gauge stations (Jan–Dec during 2008–2017); source: own elaboration

tion (WMO) recommendation in the whole basin was calculated and for rainfall intensities of 2–5 mm, 5–10 mm, 10–20 mm and >20 mm these are 25.3%, 25.2%, 28% and 21.5% respectively. As presented, rainfall is the most frequent in the intensity class of 10–20 mm.

In the long-term evaluation of hydrological trends, including 290 floods in the study area from 1955 to 2005 by [SAMADI *et al.* 2019), the authors indicated that the peak flow in 17 flood cases from 1991 to 2005 (52% of the total floods) was over 2900 $m^3 \cdot s^{-1}$, compared to the average annual flow of 258 $m^3 \cdot s^{-1}$. This basin is vital as it supplies water for households, agriculture, and industry, as well as hydropower generation, in a highly populated area downstream.

DATA RESOURCE

This section describes rainfall products along with the ground-based rainfall data. The period of the study was chosen between 2008 and 2017, since all observation and estimation datasets were complete and available.

Observation data

Rainfall data were collected from the Khuzestan Water and Power Authority (KWPA). Daily rainfall data related to the Dez Basin were obtained from 15 rain gauge stations. The KWPA regularly conducts quality control screening of ground station data, which includes tests for extreme values, internal and spatial consistency, time-

-series graph, and double mass analysis. The study period was selected based on the availability and completeness of the rain gauge data. Coordinates of the stations are presented in Table 1.

Table 1. Geographic coordinates of observational rainfall gauge stations

Station name	Longitude (E)	Latitude (N)	Elevation (m.a.s.l)
Tireh-Doroud	49°03'00"	33°27'36"	1 450
Talazang	48°46'00"	32°49'00"	440
Dem Dez	48°27'00"	32°33'00"	525
Tanga Pang Bakhti	48°46'00"	32°56'00"	600
Silakhor Rahimabad	48°48'00"	33°46'48"	1 490
Kakolstan Abbarik	49°49'05"	33°13'48"	2 470
Sabzab Chamchit	48°57'04"	33°22'48"	1 290
Azna Aliabad	49°24'00"	33°24'00"	1 830
Azana Chamzaman	49°24'00"	33°24'00"	1 830
Darh Takht	49°22'05"	33°21'36"	1 890
Bakhti Kakolstan	49°39'08"	33°01'12"	1 780
Kazamabad Kakolstan	49°40'05"	33°09'00"	2 000
Golrod Vanae	48°34'05"	33°54'00"	2 000
Kamandan	49°25'05"	33°18'00"	1 930
Sorkhab Kashvar	48°37'05"	33°07'48"	770

Source: own elaboration.

To better describe the distribution of frequency and amount of observed rainfall in the basin, the data were categorized and presented in Figure 3. In this work, wet (occurrence) days have been disaggregated from dry days (non-occurrence) using a determined rainfall intensity threshold of 1 mm·day^{-1}. The categorized rainfall frequency and the distribution between west and east of the Dez Basin are presented in Figure 3. Based on the frequency and spatial distribution, in the east of the basin, rainfall class 5–10 mm and in the west 10–20 mm class show the highest frequency in comparison with other classes. The highest rainfall occurs in the class of more than 20 mm.

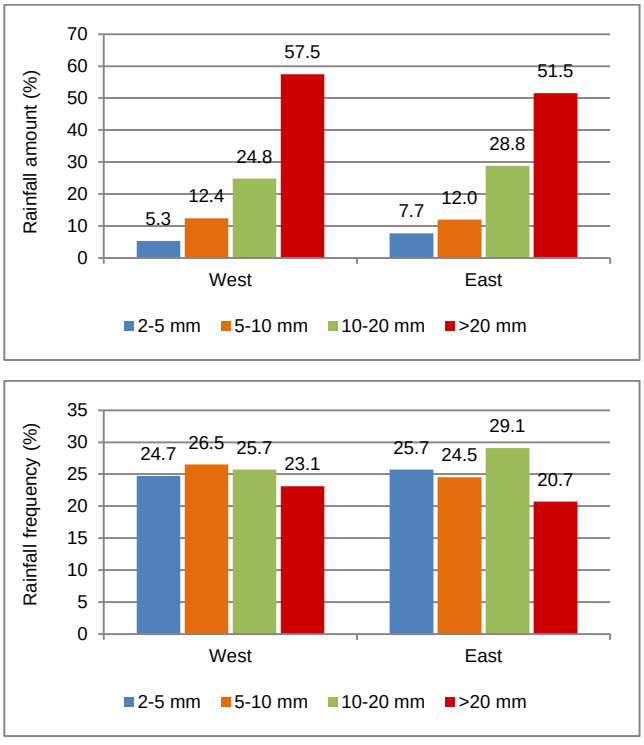

Fig. 3. Mean categorized observed rainfall amount (top) and frequency (bottom) for West and East of the Dez Basin (2008–2017); source: own elaboration

Rainfall products

The four rainfall products (PERSIANN-CCS, CMORPH, ERA5, and ERA-Interim) in this assessment are selected based on three factors: (i) structure of rainfall products including algorithm and models approach for data creation, (ii) access time, and (iii) Product Resolution.

PERSIANN satellite-based data is a rainfall estimate algorithm that uses a remote sensing algorithm working according to an artificial neural network model [HSU *et al.* 2002]. Base inputs of this model include the temperature above clouds generated by images taken from the infrared spectrum of the cloud by geosynchronous satellites, including GoEs8 and GoEs9. The images taken by geosynchronous satellites have high resolution, but the magnitude of the spatial resolution of these images is low because the distance from the ground is much higher than that of polar satellites. Using these images, the PERSIANN estimates rainfall intensity in time [HONG *et al.* 2005]. PERSIANN-CCS data used in this study included a higher generation of PERSIANN satellite-based data. The PERSIANN-CCS satellite-based data generation algorithm can classify clouds based on their height, geographical range, and texture. The presence of an algorithm with a varied threshold in the cloud classification is considered the main feature of the PERSIANN-CCS, contrary to the assumption of a constant threshold in cloud classification [SOROOSHIAN *et al.* 2000]. The varied threshold system can separate and identify each piece of cloud, and cloud pieces can be classified based on the texture, geometric properties, dynamic evolution, and overcloud height. This classification helps to assign the rainfall to pixels in each cloud so that in each case, a specific curve describes the relationship between rainfall and light temperature. PERSIANN-CCS data are available instantly with a time step of 1, 3, and 6 hours, daily, with 0.04° (degree) resolution on the following website [CHRS undated].

The CMORPH is another source of satellite-based data that have been provided by the NOAA Climate Prediction Center with a precision of 0.25° (degree) since 3 December 2002. The desired datasets can be accessed by NOAA [undated]. The CMORPH model is a motion vector based method which uses infrared images at half an hour time step to predict the precision of rainfall from inactive microwave data. The shape and duration of rainfall between microwave sensor scans is also corrected over time by a linear trend [JOYCE *et al.* 2004].

Founded in 1975, the ECMWF (European Centre for Medium-Range Weather Forecasts) is a research institute specialized in weather services. ERA-Interim is a reanalysis of the global atmosphere since 1979 to the present. The main objective of the ERA-Interim was to enhance specific aspects of the previous generation of the ECMWF, in particular hydrological cycle representation, stratospheric circulation quality, bias handling, and observation system

changes [BERRISFORD *et al.* 2009]. The reanalysis data have been created using a fixed system that is dynamically compatible with data assimilation and a model in which all available observation data are used [DIACONESCU *et al.* 2015]. The ERA-Interim data is the fourth generation of reanalysis data provided by the ECMWF. Rainfall data have been collected from 1 January 1979, to 30 June 2014, with spatial and temporal resolutions of 0.75×0.75 and 6-hour interval acc. to ECMWF [2017].

ERA5 is the latest generation of ECMWF atmospheric reanalysis products, which is available from January 1950 to the present. Furthermore, as of October 2018, it has been publicly accessible. ERA5 offers a higher spatial and temporal resolution than its predecessor ERA-Interim. Moreover, it provides hourly estimates of a large number of atmospheric, land, and oceanic climate variables. The dataset covers the surface of the Earth with a grid size of 30 km. In addition, the manifestation of tropical processes have improved dramatically in ERA5, including better representation of tropical cyclones, better global equilibrium of rainfall and evaporation, rainfall on the land and in deep equatorial regions, and more consistent sea surface temperatures and sea ice [HENNERMANN, BERRISFORD 2018]. A more detailed explanation of the ERA5 reanalysis and its difference with the previous generations can be found in [ECMWF 2017; HERSBACH, DEE 2012].

Daily accumulative rainfall was generated by adding hourly rainfall values. The gridded dataset time values are based on the Coordinated Universal Time (UTC). Due to geographic time zone difference, the time dimension was shifted according to the local time zone. In this study, the observed data (from the Khuzestan Water and Power Authority (KWPA) are considered independent from chosen rainfall products because ERA5 and ERA-Interim datasets do not include gauge rainfall measurements, and the selected stations data are not reported or collected to be used for calibration or incorporation by chosen rainfall products (Tab. 1).

METHODS

A grid-to-point comparison method was used to compare gridded rainfall products with data from 15 rain gauge stations across the study area. In the Dez River Basin with sparse rain gauge stations, the accuracy of the generated gauged-gridded data using the areal comparison method can be uncertain; therefore, the grid-to-point method was applied for the validation of rainfall products [NGUYEN *et al.* 2018]. The value of each rainfall product was interpolated at each station location using the bilinear interpolation method [FAN *et al.* 2020; HENN *et al.* 2018]. After the calculation of all performance indices, the inverse distance weighting method (IDW) was used to produce a spatial distribution of evaluation indices. The IDW is a commonly used geostatistical method in many studies [CHANG 2019], and it is accurate enough for interpolation or providing spatial distribution of different data in mountainous regions [CHEN, LIU 2012]. Due to scarcity and poor spatial distribution of the station gauges, the resolution of 0.1 degree was used. The daily, monthly, and seasonal evaluations were performed in the period between 21 March 2008 and 21 March 2017. This period was selected because of the completeness of data recorded in the rainfall station in the Dez basin. In order to examine the accuracy of rainfall products data on rainfall of varying intensity, especially heavy rains that tend to cause floods, the rainfall intensity has been categorized into four classes (1–5 mm·day^{-1}, 5–10 mm·day^{-1}, 10–20 mm·day^{-1} and >20 mm·day^{-1}) in accordance with the WMO recommendation and the modification in compliance with the frequency of local rainfall with varying intensity (Fig. 3) [BROWN 2006; CAWR 2015].

The assessment of the four rainfall products was based on the general statistical metrics, including categorial bias and rainfall detection skill following the recommendation of WMO [BROWN 2006] (categorical statistical indices) (Tab. 2). The statistical criteria include the Spearman correlation coefficient (*CC*), root mean square error (*RMSE*), and bias (Eq. 1 to Eq. 3, respectively). They were used to quantitatively compare the rainfall product relative to the rainfall observations [SHARIFI *et al*. 2016]. The Spearman rank correlation coefficient (*CC*) measures the linear monotonic association between rainfall products and observed data based on their ranks within the value range between −1 and 1 [CAWR 2015]. Bias is a representation of the systematic bias of a chosen rainfall dataset. Its positive and negative values represent over and under-estimation of the rainfall amount. *RMSE* measures the mean square error magnitude of the rainfall product. The smaller the *RMSE* value, the closer are rainfall product measurements to the observed data. To determine the rainfall detection skill, common categorical statistical indices, including the probability of detection (*POD*), false alarm rate (*FAR*), and critical success index (*CSI*), were utilized (Eq. 4 to Eq. 6, respectively) [EBERT *et al*. 2007]. *POD* represents the ratio of rainfall events that are accurately detected by a rainfall product among all actual rainfall events. *FAR* describes the ratio of events when rainfall products fail to materialize. *POD* ignores the false alarms and is sensitive to hits and should be used in conjunction with *FAR*. *CSI* represents

Table 2. Metric statistical indicators

Equation number	Formula	Optimal value
1	$Bias = \frac{\sum_{i=1}^{n}(P_i - O_i)}{n}$	0
2	$CC = \frac{\sum_{i=1}^{n}(R_i - \overline{B})(R_i - \overline{R})}{\sqrt{\sum_{i=1}^{n}(B_i - \overline{B})^2}\sqrt{\sum_{i=1}^{n}(R_i - \overline{R})^2}}$	1
3	$RMSE = \sqrt{\frac{\sum_{i=1}^{n}(P_i - O_i)^2}{n}}$	0
4	$POD = \frac{H}{H + M}$	1
5	$FAR = \frac{F}{H + F}$	0
6	$\mathrm{CSI} = \frac{H}{H + M + F}$	1

Explanation: P = data (rainfall product), O = observed data, i = event numerator, n = number of samples; for CC: R = the position of the estimates values, arranged in ascending order, B = the position of the observed values, arranged in ascending order.
Source: own elaboration.

the total proportion of rainfall events that are correctly identified by the rainfall products. *POD*, *FAR*, and *CSI* values vary from 0 to 1. The best possible score for *POD* and *CSI* is one and zero for *FAR*. Misses (*M*) describes the number of observations by the rain gauges which are not detected by the rainfall product. Hits (*H*) denotes the number of times when the occurrence of rain is correctly detected by the rainfall product. A false alarm (*F*) denotes the number of times that rain occurred, not observed by the rain gauges but detected by the rainfall product.

RESULTS

PERFORMANCE EVALUATION BASED ON DETECTION METRICS

In this section, daily and seasonal data of rainfall products were evaluated based on *FAR*, *POD* and *CSI*. It should be mentioned that in a seasonal time scale, rainfall data were not accumulated, and all daily data from a specific season were separated and analysed. Figure 4 shows the spatial distribution of *POD*, *FAR*, and *CSI* indicators. Values of these indicators are given in Figure 4, according to data recorded seasonally in Dez Basin stations. Figure 4 shows that the ERA-Interim has the highest *POD* value compared to other data. Also, Figure 5 demonstrates that this dataset performs better in seasons of autumn and winter than in spring. PERSIANN-CCS and CMORPH models show the highest *POD* in winter, compared to other seasons. Figure 4 shows that the ERA5 has the lowest *FAR* compared to other rainfall datasets. Based on Figure 5, ERA5 and ERA-Interim perform closely in autumn and winter and have a low *FAR* value, and in contrast, PERSIANN-CCS and CMORPH have the highest *FAR* in autumn and winter. Moreover, this index was found to be high in spring for all four models. The value of the *CSI* index is higher for ERA5 and ERA-Interim than PERSIANN-CCS and CMORPH (Fig. 4).

In winter and autumn, in the case of the ERA5 dataset closely followed by ERA-Interim, the *CSI* index has the highest value, whereas for PERSIANN-CCS and CMORPH, it is highest in winter and autumn in comparison to spring. Considering the spatial distribution of *POD*, *CSI*, and *FAR* indicators shown in Figure 4, it is concluded that the values of these indicators for each of the four grid datasets are such that the values of *POD* and *CSI* are reduced, and *FAR* value increased from west to east of the watershed with the increase of topographic complexity and

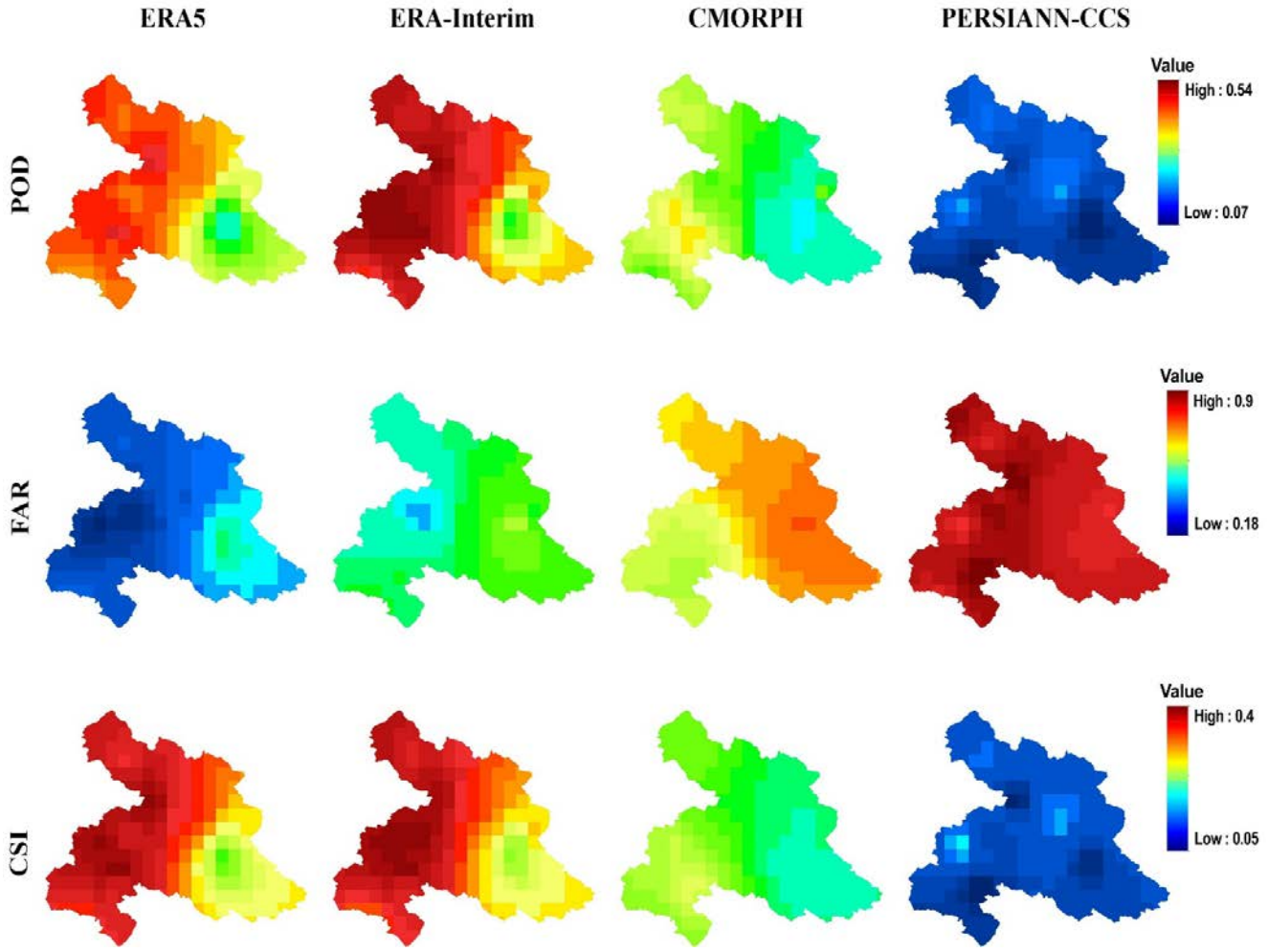

Fig. 4. Spatial distribution of probability of detection (*POD*), false alarm rate (*FAR*), and critical success index (*CSI*) for ERA5, ERA-Interim, PERSIANN-CCS, and CMORPH rainfall datasets; source: own study

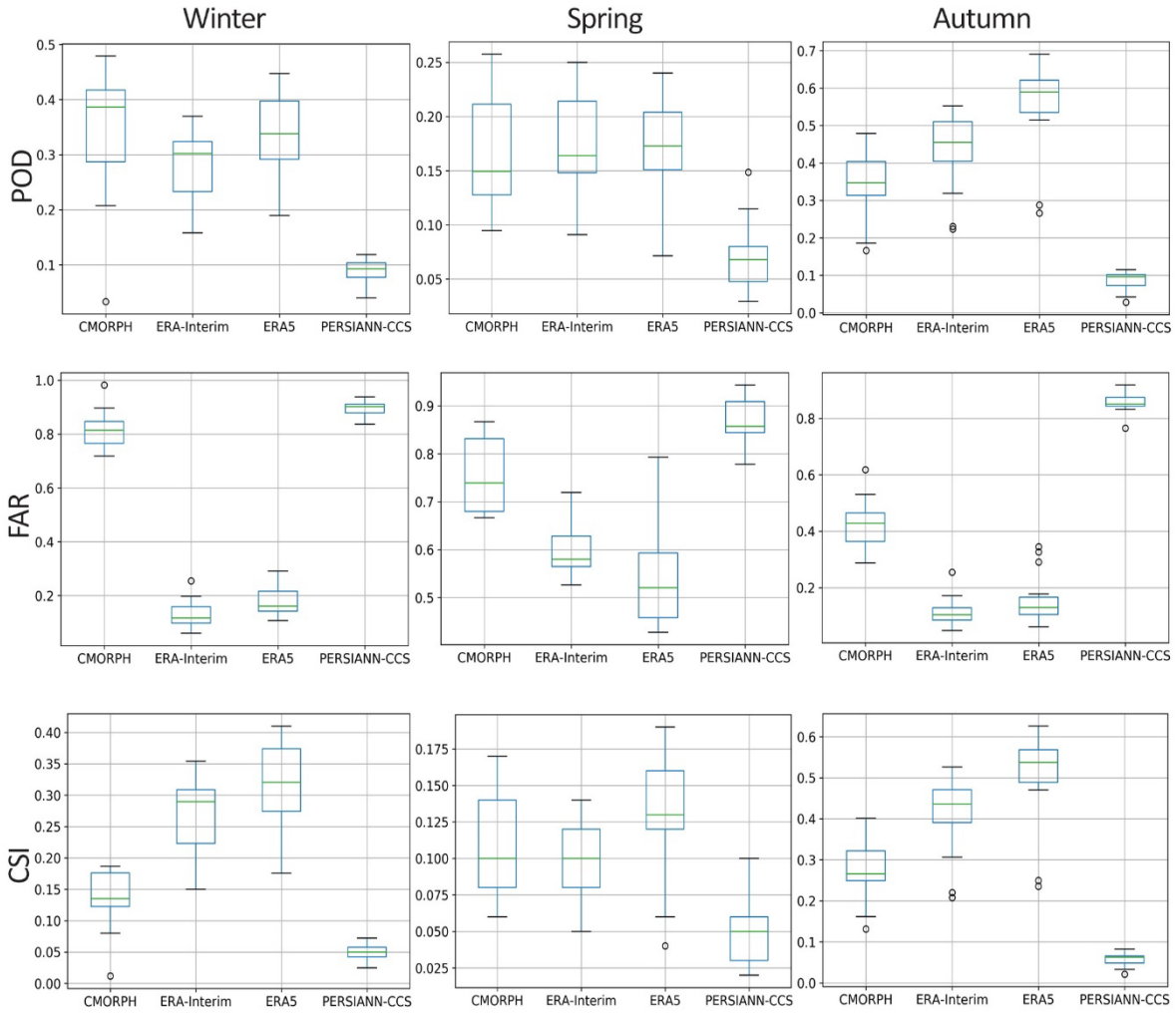

Fig. 5. Spatial variation of detection indicators in spring, winter, and autumn; *POD*, *FAR* and *CSI* as in Fig. 4; source: own study

altitude. Therefore, seemingly topographic and elevation changes reduce the quality of detection indicators in the study area.

QUANTITATIVE RAINFALL ESTIMATION SKILL

In short, a detailed assessment was performed on four grid datasets, including satellite-based rainfall reanalysis of CMORPH, PERSIANN-CCS, ERA5, and ERA-Interim on daily, monthly, and seasonal time scales. For the seasonal evaluation of these data, data on spring (21 March to 20 June), autumn (21 September to 20 December) and winter (21 December to 20 March) were reviewed; the summer was excluded from the review, considering climatic conditions of the area, as well as the lack of rainfall in this season (Fig. 2). Figure 6 shows the spatial distribution of the correlation coefficient for rainfall estimates regarding daily and monthly rainfall observations. Figure 6 illustrates that the ERA5, closely followed by ERA-Interim, shows a higher correlation with observational data at most observation stations compared to PERSIANN-CCS and CMORPH products. The spatial distribution of the correlation coefficient for the dataset in Figure 6 shows the change in the correlation coefficient of different rainfalls with topographic changes, as for rainfall in the reanalysis models of ERA5 and ERA-Interim, the correlation coefficient of rainfall reduced from west to east of the basin with increasing altitude and topographic complexity. This process is reversed for rainfall in the PERSIANN-CCS model such that the correlation coefficient increased from west to east.

According to the spatial distribution of correlation coefficients on a monthly scale (Fig. 6), it was found that on the monthly scale like the daily scale, the ERA5 model had a higher correlation than that of other rainfall products. So, for ERA5, ERA-Interim, PERSIANN-CCS, and CMORPH models, the maximum correlation on the monthly scale is equal to 0.93, 0.92, 0.64 and 0.52, respectively.

Figures 7 and 8 show the values of statistical indicators for all stations on a daily and seasonal basis for all datasets. According to the daily data, Figure 7 shows varied bias values at all stations ranging from 0.56 to –1.6 mm. They indicate the underestimation of rainfall relative to observations for ERA-Interim, PERSIANN-CCS and CMORPH and overestimation by the ERA5 product which can be attributed to the mountainous area of the Dez Basin and presence of an orographic effect that is consistent with results of [MOAZAMI *et al.* 2013] who showed the orographic effect on varied bias near Zagros Mountains. At the same time, ERA5 with a mean bias of 0.1 mm, *RMSE*

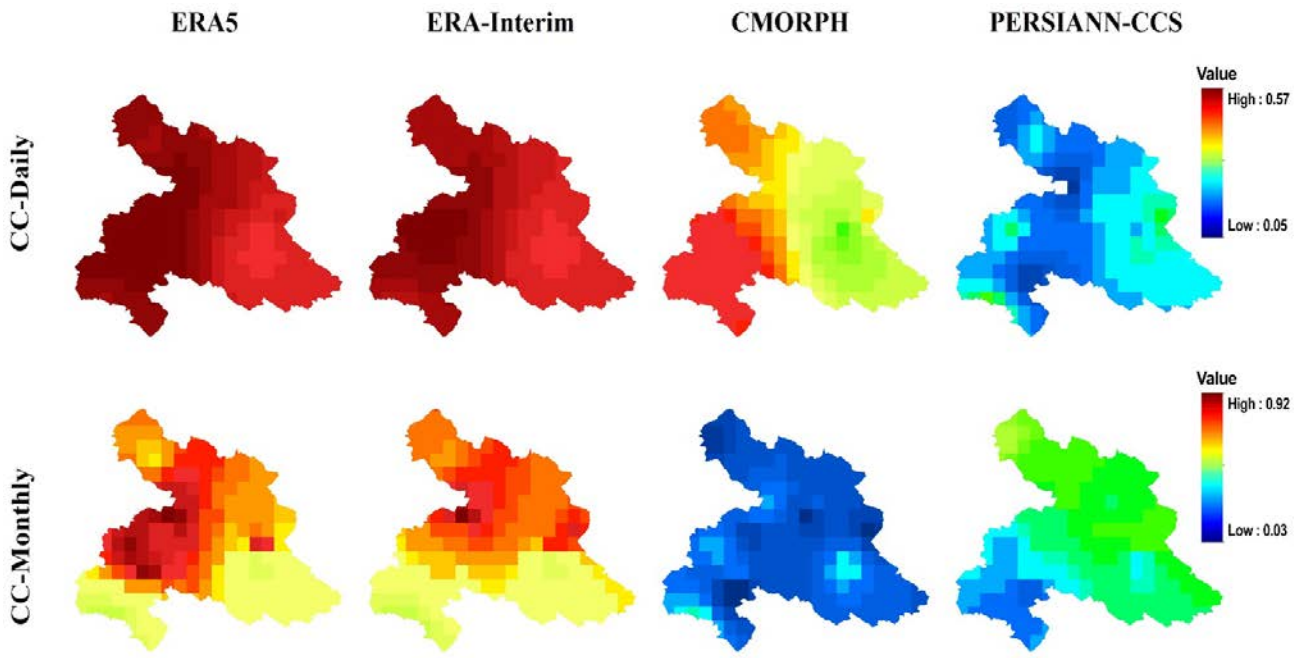

Fig. 6. Spatial distribution of daily and monthly correlation coefficient (*CC*) for 2008–2017; source: own study

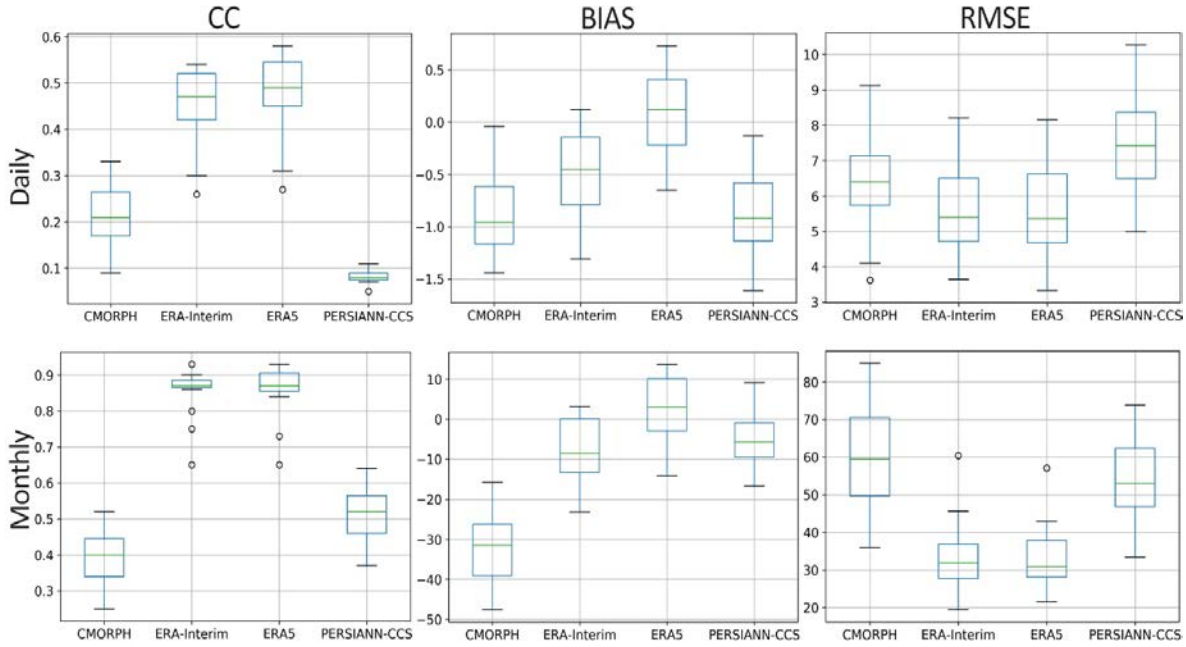

Fig. 7. Metric indicators of rainfall estimates on a daily and monthly scale; *CC* = correlation coefficient, *RMSE* = root mean square error; source: own study

of (5.49 mm), and *CC* of (0.47) provide a better estimate of the daily rainfall than ERA-Interim, PERSIANN-CCS, and CMORPH.

The study of different statistics and PERSIANN-CCS data has shown the high uncertainty of rainfall on a daily scale in this basin. Figure 7 shows different statistical values on the monthly scale for each grid rainfall dataset. Based on these values, the performance of PERSIANN-CCS and CMORPH has significantly changed compared to the daily scale. It indicates that PERSIANN-CCS and CMORPH perform better in estimating monthly rainfall than daily rainfall. Meanwhile, ERA5 and ERA-Interim, with *CC* of 0.86 and 0.85 respectively, have shown a better estimation than PERSIANN-CCS and CMORPH on a monthly scale. Figure 8 with data for spring, autumn, and winter shows that the four datasets (PERSIANN-CCS, CMORPH, ERA5, and ERA-Interim) had no acceptable performance in the spring season, and the results of the daily rainfall estimate in this season showed high uncertainty based on all four datasets. Considering the climatic and geographical situation of the basin in spring, as well as the extreme amount of rainfall in this season, the poor performance of these products is understandable.

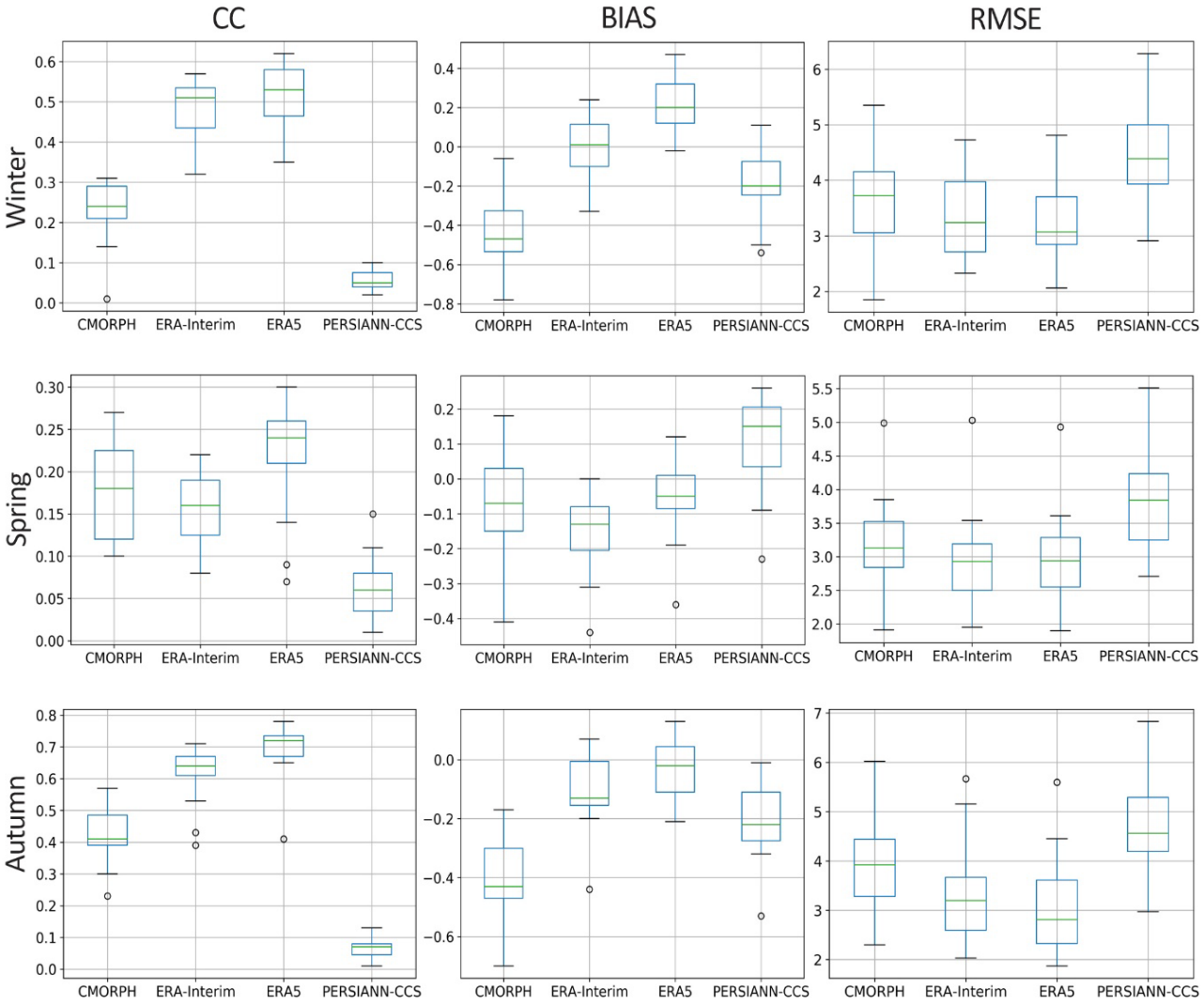

Fig. 8. Metric indicators of rainfall estimates in the winter, spring, and autumn; source: own study

Furthermore, Figure 8 shows the evaluation of all four datasets in autumn. As it was discussed, ERA5 has a better estimate of rainfall in this season compared to other products. The PERSIANN-CCS dataset with the lowest correlation at most stations and mean *RMSE* of 3.84 mm had less precision than other models for the spring season. At the same time, ERA5 with higher mean *CC* and lower *RMSE* value performs better than other datasets in this season. The results of comparisons performed between all four datasets in winter, presented in Figure 8, have shown that similarly to autumn, ERA5 with a maximum value of *CC* (0.622) has better performance than the other datasets. ERA5 generally overestimates the rainfall value in winter, while, the bias value has always been negative for PERSIANN-CCS and CMORPH at all stations in this season.

The spatial distribution of bias based on the rainfall of varying intensity is presented in Figure 9. In the rainfall class 1–5 mm·day^{-1}, ERA-Interim with an average bias of –0.17 has the best performance and then ERA5, PERSIANN-CCS, and CMORPH with an average bias of 0.9, –1.7 and –3.05. Interestingly, the values of all products except ERA5 underestimate the rainfall value. In the 5–10 mm·day^{-1} rainfall class, from best to worst, the average bias values for ERA5, ERA-Interim, PERSIANN-CCS, and CMORPH are –0.9, –2.2.7, –5.8 and –6.7 respectively. It actually shows the underestimation in all products. As shown in Figure 9, the bias value in the 1–10 mm·day^{-1} rainfall class (first two classes) for the ERA5 dataset tends to change from overestimation to underestimation as we go from the west to the east of the watershed.

In the 10–20 mm·day^{-1} rainfall class, ERA5 outperforms all other products with an average bias value of –5.99. Average values of bias in the rainfall class >20 mm·day^{-1} have significantly deteriorated, and in this class, ERA5 with a mean bias value of –17.8 performs best. As shown in Figure 9, the bias values in all rainfall classes decrease from west to east, which, as noted in previous sections, is associated with an increased topographic complexity and elevation in the region. The performance of PERSIANN-CCS, followed by CMORPH datasets, is the worst in all classes, while the performance of the other products is relatively good for rainfall classes ranging from 1 to 20 mm·day^{-1}. In the 1–20 mm·day^{-1} rainfall class, the ERA5 dataset provided acceptable accuracy, but in the rainfall class above 20 mm·day^{-1}, the performance decreased significantly and the results were unreliable.

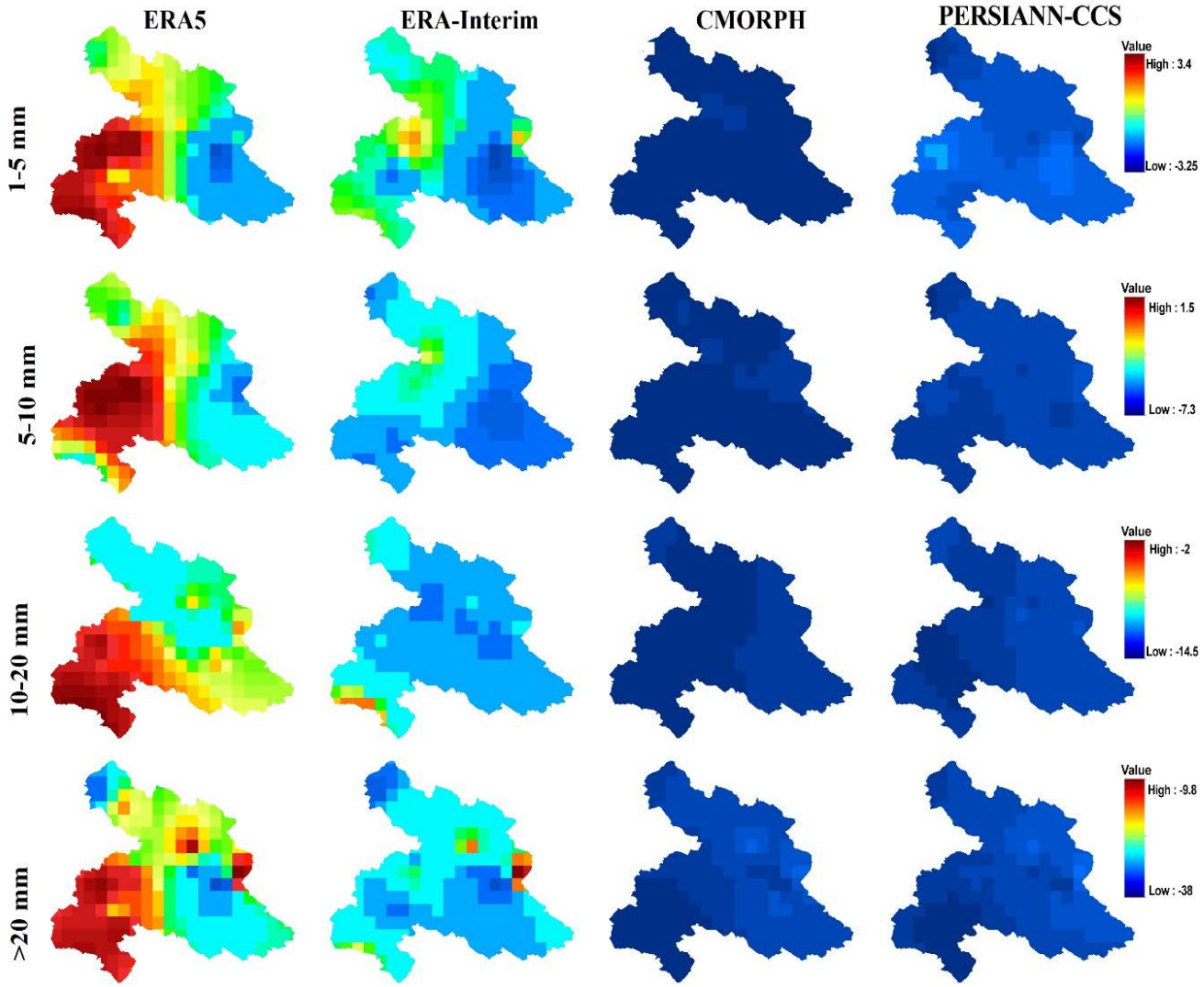

Fig. 9. Spatial distribution of bias values based on the rainfall of varying intensity; source: own study

DISCUSSION

The comparison of data on the estimated daily temporal pattern of rainfall with those of PERSIANN-CSS, CMORPH, ERA5, and ERA-Interim collected from the stations was based on three detection indicators, including false alarm rate (*FAR*), critical success index (*CSI*) and probability of detection (*POD*). The results of comparison regarding the spatial distribution of the indicators (Fig. 4) showed a significant relationship between a topographic complexity and performance of the mentioned datasets. The performance of rainfall products is generally poor in high elevation regions. This phenomenon is consistent with the findings of studies done by DERIN and YILMAZ [2014] and ZAMBRANO-BIGIARINI *et al*. [2017]. In the eastern part of the basin with a higher topographic complexity, ERA5, ERA-Interim, CMORPH, and PERSIANN-CSS showed the value of *FAR* more than 35%, 46%, 74%, and 89% respectively, while *POD* and *CSI* were reduced significantly. Among all datasets, PERSIANN-CCS with *FAR* variation range between 85% and 91 showed the lowest skill in the daily temporal pattern estimation of rainfall at all stations of the Dez River Basin, while the ERA5 as the best dataset showed the range of 18% to 43% for the same indicator all over the basin. Further analysis showed that in addition to the topography, the behaviour of each dataset has significantly changed in particular seasons. The performance of ERA5 regarding the temporal pattern estimation in autumn and winter is substantially higher than the others, whereas *FAR* is reduced to less than 20% while the PERSIANN-CSS and CMORPH showed *FAR* higher than 89% and 81%, respectively. In the autumn and winter, the *POD* variation range for ERA5 and ERA-Interim was between 42% and 51%, while the range was less than 20% for other products. In spring, the performance of all datasets is dramatically reduced so that the range of variation in all indicators increases (Fig. 5). High-intensity rainfall is common in the southwestern Zagros Mountains in spring [ALIJANI HARMAN 1985]. In mountainous regions, most of the rainfall occurs in spring due to upslope convection and especially in the southern Zagros Mountains due to the monsoonal intrusion [ALIJANI *et al*. 2008]. Therefore, particular territorial atmospheric conditions that induce these types of rainfall are not properly represented by the rainfall products.

Table 3. Comparison between the results of the current study and other studies

Reference	Study area	Period	*CC*	*RMSE*	*POD*	Bias
This study	Dez Basin, Iran	2008–2017	0.62	3.7–8.2	0.4	–0.35
SATGÉ *et al*. [2020]	West Africa	2000–2004	0.65	–	–	0.3–0.8
YAO *et al.* [2020]	China	1980–2014	0.81	1.13	–	0.47
XU *et al.* [2019]	Canada, Northern Great Plains	2002–2015	0.71	2.78	–	0.11
TAN and SANTO [2018]	Malaysia	2014–2016	0.5–0.6	12.94–14.93	0.86–0.89	–
HÉNIN *et al*. [2018]	Iberian Peninsula	2000–2008	0.23–0.42	4–17	–	–0.3
LIU *et al*. [2018]	Mainland China	1980–2012	0.82	62%	–	0.14
WONG *et al*. [2017]	Canada	1979–2012	0.49–0.56	3.65–5.12	–	–1.2–1.0
WANG *et al.* [2017]	Mekong River Basin, Thailand	2016	0.57	–	0.72	
YUAN *et al.* [2017]	Chindwin River Basin, Myanmar	2016	0.22–0.32	9.1–24.7	0.12–0.21	

Explanations: *CC* = Spearman correlation coefficient, *RMSE* = root mean square error, *POD* = probability of detection, bias = the difference between this estimator's expected value and the true value of the parameter being estimated.
Source: TAN and DUAN [2017] and TAN and SANTO [2018], modified.

The spatial distribution of *FAR* for all datasets have shown values higher than 50%, and *POD* decreased to less than 20% for all datasets. This means that the performance of all datasets in the transition from dry to wet months is better than in the transition from wet to dry months. The results of the study suggest that the ERA5 has the best performance regarding the estimation of the temporal rainfall pattern. All datasets had better performance in regions with less topographic complexity and during winter and autumn seasons.

Similarly to the detection metrics, statistical metrics of the datasets show the same pattern concerning the topographic variation. As shown in Figure 9, the accuracy of rainfall products deteriorates, moving from west to east of the basin, due to the presence of Zagros slopes. Furthermore, the performance of reanalysis datasets tends to be better compared to the satellite-based products. The spatial distribution of the correlation coefficient related to daily data indicated that the ERA5 has a much higher correlation than the PERSIANN-CSS and the CMORPH (Fig. 6). In the monthly time scale, the correlation coefficient of all datasets significantly improved together with the ERA5 and ERA-Interim variation ranges. Similar to the daily time scale, the correlation of data sets reduced in areas of higher elevation and more topographic variation. Generally, all datasets were more reliable and had better performance on monthly and seasonal time scales. Rainfall in wet seasons was estimated better than in dry seasons. Among the datasets, ERA5 and ERA-Interim showed the best rainfall estimate, whereas the CMORPH followed by the PERSIANN-CCS presented the weakest performance.

To compare the performance of ERA5 data worldwide, we updated and adopted the table used by TAN and DUAN [2017] (Tab. 3). Generally, rainfall products with the correlation coefficient of more than 0.7 and a relative bias ranging from –10% to +10% are regarded as dependable sources of rainfall data [CONDOM *et al*. 2011]. Based on the results from studies by WONG *et al*. [2017], HÉNIN *et al*. [2018], LIU *et al*. [2018], XU *et al*. [2019], SATGÉ *et al*. [2020], YAO *et al*. [2020], a strong correlation can be found in China between the ERA5, ERA-Interim and observation gauges [LIU *et al.* 2018; YAO *et al.* 2020], whereas a weak correlation ($CC < 0.5$) is reported in the Iberian Peninsula [HÉNIN *et al.* 2018]. Generally, the average correlation between ERA5 and ERA-Interim data and rainfall observation stations is between 0.5 and 0.7; therefore, additional effort is needed to enhance the algorithms used in ERA data series as a rainfall product.

CONCLUSIONS

This paper aimed to study the possibility of using rainfall products as new sources of rainfall data with the desired length of time series and reliable spatial distribution suitable for the hydrological application. Hence, the spatio-temporal assessment of four rainfall products, including PERSIAN-CSS, CMORPH, ERA5, and ERA-Interim, was conducted over the Dez River Basin of a high topographic variation on a daily, monthly and seasonal time scales in 2008–2017. Readings from the rain gauge stations were taken as reference. To determine their capabilities, several statistical parameters were used, including temporal pattern (*POD*, *FAR*, CSI) and the quantity (*CC*, *RMSE*, and bias (continuous and categorial)) of the rainfall. These are commonly applied in hydro-climatic studies. Considering the results of the study, the study led to the following conclusions.

Generally, the ERA5 and ERA-Interim perform better than the satellite-based rainfall products (PERSIANN-CCS, CMORPH), and the PERSIANN-CCS followed by the CMORPH have the worst performance in all assessments. However, the spatial variability of daily rainfall was not well reflected by rainfall products, particularly in the high-elevation eastern parts of the basin. In contrast, all rainfall products display adequate performance in monthly rainfall measurements. Also, the weak correlation between rainfall products and the rainfall gauges at a daily scale has demonstrated that additional enhancement and reforms should be carried out in rainfall product algorithms.

The ERA5 and ERA-Interim perform better during autumn and winter than the satellite-based products, while all rainfall products were poorly estimated during spring in daily rainfall measurements. This means that the performance of all datasets in the transition from dry to wet months is better than in the transition from wet to dry months.

The ERA5, with a mean CSI value of about 33% and a mean *FAR* value of 29%, indicates better rainfall detection skill than other products. On the other hand, satellite-based products have a high *FAR* in all seasons. The ERA5

has a high capability to capture the temporal pattern of rainfall during fall and winter. The ERA5 and ERA--Interim perform closely to each other in the selected region; however, the results indicate that the ERA5 dataset outperforms ERA-Interim in most indicators, which reflects the latest improvement in the ECMWF data series.

Due to the importance of heavy rainfall prediction for the flood hazard management, the rainfall has been classified based on its intensity. In the 2–20 mm·day^{-1} rainfall class, the ERA5 dataset provides reasonable accuracy, but in the rainfall class above 20 mm, the performance of all products decreases significantly, and the results are unreliable. Therefore, any evaluation performed based on data from the rainfall class above 20 mm·day^{-1} should be used with caution, especially in rainfall-runoff models.

All of the chosen rainfall products tend to underestimate the rainfall value except the ERA5 dataset. These results could provide a better estimation and more realistic future evaluation.

The major changes of the slope elevation of the Zagros Mountains in the east of the Dez Basin provide a suitable condition for the development of convection clouds that cause heavy rainfall in the area. These outcomes can lead to changes in bias values of rainfall products, increase the false alarm ratio and reduce the skill measure for rainfall variations. There is a significant relationship between a topographic complexity and the performance of the datasets; in the future investigation, the relationship between the rainfall products pattern and topographic variables, including slope, elevation, and distance from the sea, should be examined in this basin.

Regardless of the ERA5 moderate performance at the daily time scale because of latent in data availability, it is not a good candidate for the real-time application. Although this weakness translates into the fundamental strength of the satellite-based products, as discussed in previous sections, the study area is flood-prone, and the lack of the adequate observed daily rainfall is one of the main challenges for the proper setup of rainfall–runoff models; therefore, a hydrological assessment of rainfall products should be considered in the future research.

These findings will be useful for the rainfall product development and can provide an obvious insight for the future investigation. Additionally, it can draw a clear picture of alternative and supplement rainfall observation alternatives for hydrological applications, in particular, in areas that suffer from the lack of sufficient data or scattered stations.

Finally, it should be mentioned that the results of this study were obtained according to the total rainfall estimated by rain gauge stations distributed in the Dez Basin. In general, the study provided a comprehensive evaluation of PERSIANN-CCS, CMORPH, ERA5, and ERA-Interim grid data on different time scales. The study offers a reasonable basis for using these rainfall datasets in a highly topographically heterogeneous and data-scarce basins, as well as it provides a useful insight for the hydrologists to determine errors in these datasets.

ACKNOWLEDGMENT

We wish to express our gratitude to the Shahid Chamran University of Ahvaz, Faculty of Water Science Engineering, Department of Water and Environment for their support and much appreciated guidance.

REFERENCES

ALIJANI B., HARMAN J.R. 1985. Synoptic climatology of precipitation in Iran [online]. Annals of the Association of American Geographers. Vol. 75. No. 3 p. 404–416. [Access 5.03.2020]. Available at: https://www.jstor.org/stable/2562643

ALIJANI B., O'BRIEN J., YARNAL B. 2008. Spatial analysis of precipitation intensity and concentration in Iran. Theoretical and Applied Climatology. Vol. 94. No. 1–2 p. 107–124.

BERRISFORD P., DEE D.P., POLI P., BRUGGE R., FIELDING M., FUENTES M., KÅLLBERG P.W., KOBAYASHI, S., UPPALA S., SIMMONS A. 2009. The ERA-Interim Archive Version 2.0 [online]. ERA report series. [Access 5.03.2020]. Available at: https://www.ecmwf.int/en/elibrary/8174-era-interim-archive-version-20

BROWN J.E.M. 2006. An analysis of the performance of hybrid infrared and microwave satellite precipitation algorithms over India and adjacent regions. Remote Sensing of Environment. Vol. 101. No. 1 p. 63–81. DOI 10.1016/j.rse.2005.12.005.

CAWR 2015. Forecast verification methods across time and space scales [online]. WWRP/WGNE Joint Working Group on Forecast Verification Research. Center for Advanced Water Research p. 1–48. [Access 11.03.2020]. Available at: https://www.cawcr.gov.au/projects/verification/#Introduction

CHANG K. 2019. Introduction to Geographic Information Systems. 9th ed. McGraw-Hill Higher Education. ISBN 1259929647 pp. 464.

CHEN F.-W., LIU C.-W. 2012. Estimation of the spatial rainfall distribution using inverse distance weighting (IDW) in the middle of Taiwan. Paddy and Water Environment. Vol. 10. No. 3 p. 209–222. DOI 10.1007/s10333-012-0319-1.

CHEN H., YONG B., SHEN Y., LIU J., HONG Y., ZHANG J. 2020. Comparison analysis of six purely satellite-derived global precipitation estimates. Journal of Hydrology. Vol. 581, 124376. DOI 10.1016/j.jhydrol.2019.124376.

CHRS undated. PERSIANN-CCS [online]. Center for Hydrometeorology and Remote Sensing Data Portal. [Access 11.04.2020]. Available at: https://chrsdata.eng.uci.edu/

CONDOM T., RAU P., ESPINOZA J.C. 2011. Correction of TRMM 3B43 monthly precipitation data over the mountainous areas of Peru during the period 1998-2007. Hydrological Processes. Vol. 25. No. 12 p. 1924–1933. DOI 10.1002/hyp.7949.

DARAND M., AMANOLLAHI J., ZANDKARIMI S. 2017. Evaluation of the performance of TRMM Multi-satellite Precipitation Analysis (TMPA) estimation over Iran. Atmospheric Research. Vol. 190 p. 121–127. DOI 10.1016/j.atmosres.2017.02.011.

DARAND M., KHANDU K. 2020. Statistical evaluation of gridded precipitation datasets using rain gauge observations over Iran. Journal of Arid Environments. Vol. 178, 104172. DOI 10.1016/j.jaridenv.2020.104172.

DERIN Y., YILMAZ K.K. 2014. Evaluation of multiple satellite-based precipitation products over complex topography. Journal of Hydrometeorology. Vol. 15. No. 4 p. 1498–1516.

DIACONESCU E.P., GACHON P., SCINOCCA J., LAPRISE R. 2015. Evaluation of daily precipitation statistics and monsoon onset/retreat over western Sahel in multiple data sets. Climate Dynamics. Vol. 45. No. 5–6 p. 1325–1354. DOI 10.1007/s00382-014-2383-2.

EBERT E.E., JANOWIAK J.E., KIDD C. 2007. Comparison of near-real-time precipitation estimates from satellite observations

and numerical models. Bulletin of the American Meteorological Society. Vol. 88. No. 1 p. 47–64.

ECMWF 2017. ERA5 data documentation [online]. Reading. European Centre for Medium-Range Weather Forecasts. [Access 10.04.2020]. Available at: https://confluence.ecmwf.int/display/CKB/ERA5%3A+data+documentation

FAN M., XU J., CHEN Y., LI W. 2020. Simulating the precipitation in the data-scarce Tianshan Mountains, Northwest China based on the Earth system data products. Arabian Journal of Geosciences. Vol. 13. No. 14 p. 637. DOI 10.1007/s12517-020-05509-1.

HÉNIN R., LIBERATO M.L.R., RAMOS A.M., GOUVEIA C.M. 2018. Assessing the use of satellite-based estimates and high-resolution precipitation datasets for the study of extreme precipitation events over the Iberian Peninsula. Water. Vol. 10. No. 11 p. 1688. DOI 10.3390/w10111688.

HENN B., NEWMAN A.J., LIVNEH B., DALY C., LUNDQUIST J.D. 2018. An assessment of differences in gridded precipitation datasets in complex terrain. Journal of Hydrology. Vol. 556 p. 1205–1219. DOI 10.1016/j.jhydrol.2017. 03.008.

HENNERMANN K., BERRISFORD P. 2018. What are the changes from ERA-Interim to ERA5 [online]. Reading. European Centre for Medium-Range Weather Forecasts. [Access 11.03.2020]. Available at: https://confluence.ecmwf.int/pages/viewpage.action?pageId=74764925

HERSBACH H., DEE D. 2012. ERA5 reanalysis is in production [online]. ECMWF. ECMWF Newsletter. No. 147 [Access 10.04.2020]. Available at: https://www.ecmwf.int/en/newsletter/147/news/era5-reanalysis-production

HONG Y., HSU K.-L., SOROOSHIAN S., GAO X. 2005. Precipitation estimation from remotely sensed imagery using an artificial neural network cloud classification system. Journal of Applied Meteorology. Vol. 43. No. 12 p. 1834–1853. DOI 10.1175/jam2173.1.

HSU K.-L., GAO X., SOROOSHIAN S., GUPTA H.V. 2002. Precipitation estimation from remotely sensed information using artificial neural networks. Journal of Applied Meteorology. Vol. 36. No. 9 p. 1176–1190. DOI 10.1175/1520-0450(1997)036<1176:pefrsi>2.0.co;2.

ISOTTA F.A., VOGEL R., FREI C. 2015. Evaluation of European regional reanalyses and downscalings for precipitation in the Alpine region. Meteorologische Zeitschrift. Vol. 24. No. 1 p. 15–37. DOI 10.1127/metz/2014/0584.

JOYCE R.J., JANOWIAK J.E., ARKIN P.A., XIE P. 2004. CMORPH: A method that produces global precipitation estimates from passive microwave and infrared data at high spatial and temporal resolution. Journal of Hydrometeorology. Vol. 5. No. 3 p. 487–503. DOI 10.1175/1525-7541(2004)005<0487:camtpg>2.0.co;2.

KHOSHCHEHREH M., GHOMESHI M., SHAHBAZI A. 2020. Hydrological evaluation of global gridded precipitation datasets in a heterogeneous and data-scarce basin in Iran. Journal of Earth System Science. Vol. 129. No. 1, 201. DOI 10.1007/s12040-020-01462-5.

KIANI M., LASHKARI H., GHAEMI H. 2019. The effect of Zagros Mountains on rainfall changes of Sudanese low pressure system in western Iran. Modeling Earth Systems and Environment. Vol. 5. No. 4 p. 1769–1779. DOI 10.1007/s40808-019-00631-w.

KUCERA P.A., EBERT E.E., TURK F.J., LEVIZZANI V., KIRSCHBAUM D., TAPIADOR F.J., LOEW A., BORSCHE M. 2013. Precipitation from space: Advancing earth system science. Bulletin of the American Meteorological Society. Vol. 94. No. 3 p. 365–375. DOI 10.1175/BAMS-D-11-00171.1.

LIU Z., LIU Y., WANG S., YANG X., WANG L., BAIG M.H.A., WENFENG C., WANG Z. 2018. Evaluation of spatial and temporal performances of ERA-Interim precipitation and temperature in mainland China. Journal of Climate. Vol. 31. No. 11 p. 4347–4365. DOI 10.1175/JCLI-D-17-0212.1.

MOAZAMI S., GOLIAN S., HONG Y., SHENG CH., KAVIANPOUR M.R. 2016. Comprehensive evaluation of four high-resolution satellite precipitation products under diverse climate conditions in Iran. Hydrological Sciences Journal. Vol. 61. No. 2 p. 420–440. DOI 10.1080/02626667.2014.987675.

MOAZAMI S., GOLIAN S., KAVIANPOUR M.R., HONG Y. 2013. Comparison of PERSIANN and V7 TRMM multi-satellite precipitation analysis (TMPA) products with rain gauge data over Iran. International Journal of Remote Sensing. Vol. 34. No. 22 p. 8156–8171. DOI 10.1080/01431161.2013.833360.

NGUYEN T.H., MASIH I., MOHAMED Y.A., VAN DER ZAAG P. 2018. Validating rainfall-runoff modelling using satellite-based and reanalysis precipitation products in the Sre Pok catchment, the Mekong River Basin. Geosciences. Vol. 8. No. 5, 164 p. 1–20. DOI 10.3390/geosciences8050164.

NOAA undated. Index of /precip/CMORPH_V1.0 [online]. Washington, DC. National Oceanic and Atmospheric Administration. Weather Service Climate Prediction Center. [Access date: 2020/02]. Available at: https://ftp.cpc.ncep.noaa.gov/precip/CMORPH_V1.0/

NOGUEIRA M. 2020. Inter-comparison of ERA-5, ERA-interim and GPCP rainfall over the last 40 years: Process-based analysis of systematic and random differences. Journal of Hydrology. Vol. 583, 124632. DOI 10.1016/j.jhydrol.2020. 124632.

PEEL M.C., FINLAYSON B.L., MCMAHON T.A. 2007. Updated world map of the Köppen-Geiger climate classification. Hydrology and earth system sciences discussions. Vol. 4. No. 2 p. 439–473. DOI 10.5194/hess-11-1633-2007.

PREIN A.F., GOBIET A. 2017. Impacts of uncertainties in European gridded precipitation observations on regional climate analysis. International Journal of Climatology. Vol. 37. No. 1 p. 305–327. DOI 10.1002/joc.4706.

RAZIEI T. 2016. Köppen-Geiger climate classification of Iran and investigating its changes during 20th century. Journal of the Earth and Space Physics. Vol. 43 p. 419–440. DOI 10.22059/jesphys.2017.58916.

SAMADI A., SADROLASHRAFI S.S., KHOLGHI M.K. 2019. Development and testing of a rainfall-runoff model for flood simulation in dry mountain catchments: A case study for the Dez River Basin. Physics and Chemistry of the Earth, Parts A/B/C. Vol. 109 p. 9–25. 10.1016/j.pce.2018.07.003

SATGE F., DEFRANCE D., SULTAN B., BONNET M.-P., SEYLER F., ROUCHE N., PIERRON F., PATUREL J.-E. 2020. Evaluation of 23 gridded precipitation datasets across West Africa. Journal of Hydrology. Vol. 581, 124412. DOI 10.1016/j.jhydrol.2019. 124412.

SHARIFI E., STEINACKER R., SAGHAFIAN B. 2016. Assessment of GPM-IMERG and other precipitation products against gauge data under different topographic and climatic conditions in Iran: Preliminary results. Remote Sensing. Vol. 8. No. 2, 135 p. 1–24. DOI 10.3390/rs8020135.

SKOK G., ŽAGAR N., HONZAK L., ŽABKAR R., RAKOVEC J., CEGLAR A. 2016. Precipitation intercomparison of a set of satellite- and raingauge-derived datasets, ERA Interim reanalysis, and a single WRF regional climate simulation over Europe and the North Atlantic. Theoretical and Applied Climatology. Vol. 123. No. 1–2 p. 217–232. DOI 10.1007/s00704-014-1350-5.

SOROOSHIAN S., HSU K.-L., GAO X., GUPTA H.V., IMAM B., BRAITHWAITE D. 2000. Evaluation of PERSIANN system satellite-based estimates of tropical rainfall. Bulletin of the

American Meteorological Society. Vol. 81. No. 9 p. 2035–2046. DOI 10.1175/1520-0477(2000)081<2035:EOPSSE>2.3.CO;2.

SUSENO D.P.Y., YAMADA T.J. 2020. Simulating flash floods using geostationary satellite-based rainfall estimation coupled with a land surface model. Hydrology. Vol. 7. No. 1 p. 1–12. DOI 10.3390/hydrology7010009.

TAN M.L., DUAN Z. 2017. Assessment of GPM and TRMM precipitation products over Singapore. Remote Sensing. Vol. 9. No. 7, 720. DOI 10.3390/rs9070720.

TAN M.L., SANTO H. 2018. Comparison of GPM IMERG, TMPA 3B42 and PERSIANN-CDR satellite precipitation products over Malaysia. Atmospheric Research. Vol. 202 p. 63–76. DOI 10.1016/j.atmosres.2017.11.006.

TAREK M., BRISSETTE F.P., ARSENAULT R. 2020. Evaluation of the ERA5 reanalysis as a potential reference dataset for hydrological modelling over North America. Hydrology and Earth System Sciences. Vol. 24 p. 2527–2544. DOI 10.5194/hess-24-2527-2020.

WANG W., LU H., ZHAO T., JIANG L., SHI J. 2017. Evaluation and comparison of daily rainfall from latest GPM and TRMM products over the Mekong River Basin. IEEE Journal of Selected Topics in Applied Earth Observations and Remote Sensing. Vol. 10. No. 6 p. 2540–2549. DOI 10.1109/JSTARS.2017.2672786.

WESTRICK K.J., MASS C.F., COLLE B.A. 1999. The Limitations of the WSR-88D radar network for quantitative precipitation measurement over the coastal western United States. Bulletin of the American Meteorological Society. Vol. 80. No. 11 p. 2289–2298. DOI 10.1175/1520-0477(1999)080<2289:TLOTWR>2.0.CO;2.

WONG J.S., RAZAVI S., BONSAL B.R., WHEATER H.S., ASONG Z.E. 2017. Inter-comparison of daily precipitation products for large-scale hydro-climatic applications over Canada. Hydrology and Earth System Sciences. Vol. 21. No. 4 p. 2163–2185. DOI 10.5194/hess-21-2163-2017.

XU X., FREY S.K., BOLUWADE A., ERLER A.R., KHADER O., LAPEN D.R., SUDICKY E. 2019. Evaluation of variability among different precipitation products in the Northern Great Plains. Journal of Hydrology: Regional Studies. Vol. 24, 100608. DOI 10.1016/j.ejrh.2019.100608.

YAO J., CHEN Y., YU X., ZHAO Y., GUAN X., YANG L. 2020. Evaluation of multiple gridded precipitation datasets for the arid region of northwestern China. Atmospheric Research. Vol. 236, 104818. DOI 10.1016/j.atmosres.2019.104818.

YONG B., HONG Y., REN L.L., GOURLEY J.J., HUFFMAN G.J., CHEN X., WANG W., KHAN S.I. 2012. Assessment of evolving TRMM-based multisatellite real-time precipitation estimation methods and their impacts on hydrologic prediction in a high latitude basin. Journal of Geophysical Research: Atmospheres. Vol. 117. No. D9 p. n/a-n/a. DOI 10.1029/2011jd017069.

YUAN F., ZHANG L., WIN K.W.W., REN L., ZHAO CH., ZHU Y., JIANG S., LIU Y. 2017. Assessment of GPM and TRMM multi-satellite precipitation products in streamflow simulations in a data sparse mountainous watershed in Myanmar. Remote Sensing. Vol. 9. No. 3, 302. DOI 10.3390/rs9030302.

ZAMBRANO-BIGIARINI M., NAUDITT A., BIRKEL CH., VERBIST K., RIBBE L. 2017. Temporal and spatial evaluation of satellite-based rainfall estimates across the complex topographical and climatic gradients of Chile. Hydrology and Earth System Sciences. Vol. 21. No. 2 p. 1295–1320. DOI 10.5194/hess-21-1295-2017.